Matter-Wave Dark Solitons: Stochastic versus Analytical Results

S. P. Cockburn,[1] H. E. Nistazakis,[2] T. P. Horikis,[3] P. G. Kevrekidis,[4] N. P. Proukakis,[1] and D. J. Frantzeskakis[2]

[1]*School of Mathematics and Statistics, Newcastle University, Newcastle upon Tyne, NE1 7RU, United Kingdom*
[2]*Department of Physics, University of Athens, Panepistimioupolis, Zografos, Athens 15784, Greece*
[3]*Department of Mathematics, University of Ioannina, Ioannina 45110, Greece*
[4]*Department of Mathematics and Statistics, University of Massachusetts, Amherst, Massachusetts 01003-4515, USA*

(Received 8 September 2009; published 29 April 2010)

The dynamics of dark matter-wave solitons in elongated atomic condensates are discussed at finite temperatures. Simulations with the stochastic Gross-Pitaevskii equation reveal a noticeable, experimentally observable spread in individual soliton trajectories, attributed to inherent fluctuations in both phase and density of the underlying medium. Averaging over a number of such trajectories (as done in experiments) washes out such background fluctuations, revealing a well-defined temperature-dependent temporal growth in the oscillation amplitude. The *average* soliton dynamics is well captured by the simpler dissipative Gross-Pitaevskii equation, both numerically and via an analytically derived equation for the soliton center based on perturbation theory for dark solitons.

DOI: 10.1103/PhysRevLett.104.174101 PACS numbers: 03.75.Lm, 05.40.-a, 05.45.Yv

Introduction.—Atomic Bose-Einstein condensates (BECs) constitute ideal systems for studying nonlinear macroscopic excitations in quantum systems [1]. Excitations in the form of dark solitons and vortices, known to arise spontaneously at phase transitions [2,3], are features also studied in high-energy [4] and condensed-matter [5] systems, in dynamical processes [6], and through controlled engineering [7–12]. Although thermal effects revealed rapid soliton decay near the condensate edge [7,13], recent experiments at reduced temperatures ($T \ll 0.5T_c$) [9–11] found the predicted [14] oscillatory pattern for the averaged soliton trajectories.

To date, finite temperature dynamics of dark solitons have been investigated with phenomenological [15], quasiparticle scattering [16], and generalized mean-field [13] models; see also [17] for quantum effects. The former predict oscillations with increasing amplitude (''antidamping'' [14]), reproducing the average soliton trajectories to varying degrees of accuracy; however, they fail to account for the random nature of the experiments. In particular, experiments showed variations from shot to shot [9–11], with single realizations revealing the existence of dark solitons for times much longer than those for which a reproducible (or average) pattern can be generated, an effect attributed to ''preparation errors'' [9].

In this Letter we show that a spread in the trajectories of dark solitons prepared in the same manner could also arise due to the critical dependence of individual solitons on local phase or density fluctuations. Modeling the system by the stochastic Gross-Pitaevskii equation (SGPE) [18,19], we (i) calculate the spread of individual soliton trajectories *ab initio* (Fig. 1, top); (ii) demonstrate that the well-defined pattern generated by averaging over different trajectories is restricted to times much less than the longest observed trajectories (Fig. 1, bottom), consistent with experiments [9–11]; (iii) show that results based on stochastic trajectory averaging can be well captured by the dissipative GPE (DGPE) [15,20–22], with an *ab initio* damping term; (iv) derive an analytical equation for the soliton center which captures the average dynamics at low temperatures.

Stochastic dynamics.—The importance of fluctuations to the motion of solitonlike structures manifests in diverse fields such as nonlinear optics [23], condensed-matter [24], biological physics [25], and physics of the early Universe [26], with their description often meriting a stochastic formulation. For weakly interacting atomic BECs, an appropriate description of this dynamics is given by the SGPE [18,19]: this describes the condensate and lowest

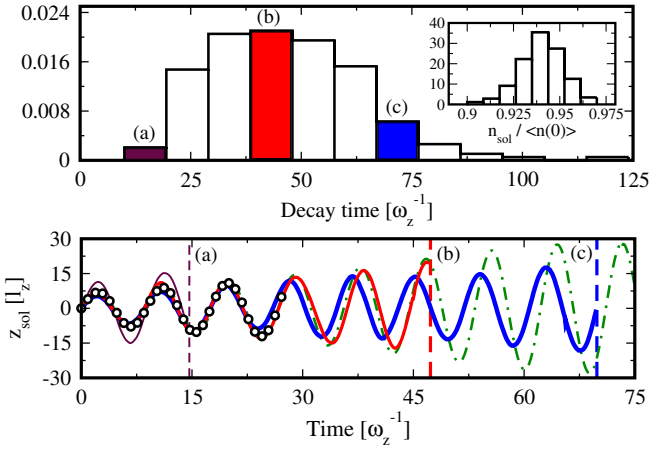

FIG. 1 (color online). Top: Normalized histograms of soliton decay times (main) and initial soliton depth, $n_{\rm sol}$, scaled to the average peak density $\langle n(0)\rangle$ (inset) (based on 200 realizations). Bottom: Individual stochastic trajectories from marked histogram bins (for as long as they are numerically tractable), ten-realization trajectory average (black circles) and DGPE trajectory (green, dash-dotted). (Parameters: $N \approx 20\,000$ ^{87}Rb atoms, $T = 175$ nK, $\omega_z = 2\pi \times 10$ Hz, $\omega_\perp = 250\omega_z$, $\mu = 395\hbar\omega_z$, $k_B T < 2\hbar\omega_\perp$, $l_z = \sqrt{\hbar/m\omega_z}$ and $|v| = 0.25c$.)

excitations in a unified manner, including both density and phase fluctuations, with irreversibility and damping arising from the coupling of such modes to a thermal particle reservoir. For the parameters of interest here (see below), the soliton dynamics occurs essentially along the axial direction, and we solve an effective 1D equation which, assuming a ''classical'' distribution for the modes and a near equilibrium thermal cloud, reads [18]

$$i\hbar\partial_t\psi = (1 - i\gamma)\left[-\frac{\hbar^2}{2m}\partial_z^2 + V(z) + g|\psi|^2 - \mu\right]\psi + \eta. \tag{1}$$

Here $g = 2a\hbar\omega_\perp$ is the effective 1D coupling strength (assuming Gaussian transverse profiles, with a the 3D scattering length and $\omega_\perp \gg \omega_z$ the transverse harmonic confinement), and $V(z) = (1/2)m\omega_z^2 z^2$ the axial confining potential. $\gamma = i\beta\hbar\Sigma^K(z, t)/4$ represents the *ab initio* determined dissipation arising due to the coupling to the thermal cloud ($\beta = 1/k_B T$). $\hbar\Sigma^K(z, t)$ is the Keldysh self-energy due to incoherent collisions between condensate and noncondensate atoms and η is a noise term with Gaussian correlations $\langle\eta^*(z, t)\eta(z', t')\rangle = 2\hbar k_B T\gamma(z, t)\delta(z - z')\delta(t - t')$ (see [18,27] for details).

Soliton experiments are modeled by letting the system equilibrate at a given temperature and then introducing a dark soliton of specified velocity v at the trap center by multiplying ψ by $\psi_{\rm sol} = \zeta\tanh(\zeta z/\xi) + i(v/c)$, where $\zeta = \sqrt{1 - (v/c)^2}$ (ξ: healing length, c: speed of sound). Although the soliton generation is identical in all realizations, fluctuations inherent in the atomic medium lead to a large variation in the imprinted soliton: The soliton speed $v/c = \sqrt{1 - n_d/n} = \cos(S/2)$ is closely related to the depth of the density minimum (n_d) and the phase slip S across it. As a result, background phase and density fluctuations upon generation should introduce a stochasticity to the initial conditions, which we find leads to a slightly asymmetric spread in the initial soliton depth (Fig. 1, inset); the ensuing trajectory is further modified by the local fluctuations during the SGPE evolution.

Soliton experiments are typically conducted in highly elongated geometries, in order to avoid dynamical instabilities [28]. Phase fluctuations in such geometries set in at a characteristic temperature T_ϕ [29], which can be much lower than the ''critical'' temperature T_c [30]. Although recent experiments [9–11] were conducted in the regime $T \ll T_\phi, T_c$, where both density and phase fluctuations are largely suppressed, soliton oscillations can still be observed in the presence of phase fluctuations ($T \gg T_\phi$), provided $T \ll T_c$. To amplify the differences between individual trajectories, we thus choose a rather deep initial soliton and realistic experimental parameters ($N \approx 20\,000$ ^{87}Rb atoms, $\omega_z = 2\pi \times 10$ Hz, $\omega_\perp = 250\omega_z$) corresponding to this intermediate regime $T_\phi \ll T \ll T_c$, for which the solitons ($\mu < 2\hbar\omega_\perp$) are dynamically stable [28]. The phase coherence length $L_\phi \approx (0.1\text{–}0.2)R$ (R: Thomas-Fermi radius), with the effective soliton ''width'' $\xi \ll L_\phi$.

Typical trajectories are shown in Fig. 1 (bottom) up to the point where the soliton can be numerically identified over the fluctuating background, which sets a decay time for each realization. We find an asymmetric distribution of decay times, with some very long-lived trajectories, as best visualized in individual trajectories from different histogram bins [labeled (a)–(c)]. Despite their differences, averaging over a sufficient number of trajectories (typically $\geq$10) washes out such sensitivity, generating an antidamped oscillatory pattern, with a temperature-dependent shift in amplitude and phase (black circles). The average trajectory is only defined up to the earliest decay time within the set of trajectories considered (here $27\omega_z^{-1}$), in analogy to the experimentally reproducible soliton dynamics being restricted to much shorter times than those of individual long-lived trajectories [9–11]. The average trajectory is practically indistinguishable from an individual trajectory from the mean decay time bin (solid red), enabling us to infer the average soliton evolution from a single trajectory with a decay time close to the mean.

Figure 2 shows the dependence of the soliton decay time on temperature (red circles) in the intermediate temperature range of noticeable antidamping: At higher T the soliton is lost to the fluctuating background, prior to executing one full oscillation, thus leading to a decrease in the width of the decay time histogram, and to smaller error bars in the mean decay time. Although our model predicts very little damping for $T \leq 100$ nK $\approx 10\%T_c$, consistent with recent pure condensate experiments [11], our results may overestimate the actual lifetimes, due to the neglected role of dynamics of the thermal cloud [13].

The DGPE vs the SGPE.—A dissipative mean-field equation similar to Eq. (1), but without a noise term, was first introduced phenomenologically [20]; in BECs this was applied to damping of excitations [21], vortex lattice growth [22,31] and dark soliton decay [15]. A numerical advantage of the DGPE (also restricting its predictive ability) is that only a single realization is needed under the assumption that trajectory-averaged properties only depend on the dissipation [shown in Fig. 2 (inset)]. The self-consistent inclusion of the mean-field potential $2g\langle|\psi|^2\rangle$ in the expression for γ generates a flattened profile around the trap center, with peaks at the condensate edges. As the soliton resides mainly within the condensate, an averaged dissipation can be extracted as $\bar{\gamma} = \int\gamma(z)dz/R$ over, e.g. $[-R/2, R/2]$. While comparison to the formula $\gamma(0) = \alpha(ma^2k_BT/\pi\hbar^2)$, with $\alpha \approx 3$ [31], reveals $\bar{\gamma}$ has a more pronounced temperature scaling, $1/2 < \alpha < 4$ yields damping comparable to $\bar{\gamma}$.

At low temperatures, the DGPE soliton oscillations are practically indistinguishable from the SGPE ones (Fig. 1, bottom), leading to similar soliton decay times (Fig. 2): in the DGPE, these are identified by the time taken for the soliton to decay to a depth comparable to the background

density fluctuations (predicted by a single SGPE run, or measured experimentally). We find good agreement for both $\gamma(z)$ and $\bar{\gamma}$, within the error bars (gray bands), with a smaller relative error at lower temperatures. We have also verified the validity of our 1D model by a direct comparison of the 1D DGPE predictions (blue hollow squares) to those of the 3D DGPE with corresponding $\bar{\gamma}$ (orange filled squares). We now provide an analytical solution for the soliton evolution within the DGPE.

Analytical results.—Upon dropping the position dependence of $\gamma(z)$ and further introducing the transformation $t \to (1+\gamma^2)t$, the 1D DGPE takes the form

$$(i-\gamma)\partial_t\psi = [-\tfrac{1}{2}\partial_z^2 + V(z) + |\psi|^2 - \mu]\psi, \qquad (2)$$

where the density $|\psi|^2$, length, time and energy are, respectively, measured in units of $(2a)^{-1}$, $l_\perp = \sqrt{\hbar/m\omega_\perp}$, $\omega_\perp^{-1}$, and $\hbar\omega_\perp$, and $V(z) = (1/2)\Omega^2 z^2$, with $\Omega = \omega_z/\omega_\perp \ll 1$. We seek a solution of Eq. (2) in the form $\psi(z,t) = \psi_b(z,t)e^{-i\theta(t)}v(z,t)$, where $\psi_b(z,t)$ and $\theta(t)$ denote the background amplitude and phase, respectively, while the dark soliton $v(z,t)$ is governed by

$$i\partial_t v + \frac{1}{2}\partial_z^2 v - \psi_b^2(|v|^2-1)v = -\frac{\partial_z\psi_b}{\psi_b}\partial_z v + \gamma\partial_t v. \qquad (3)$$

Assuming that the condensate dynamics involves a fast relaxation scale to the ground state and that the dark soliton evolves on top of this, in the Thomas-Fermi limit, and rescaling $t \to \mu t$, $z \to \sqrt{\mu}z$, we obtain a perturbed nonlinear Schrödinger equation:

$$i\partial_t v + \tfrac{1}{2}\partial_z^2 v - (|v|^2-1)v = P(v), \qquad (4)$$

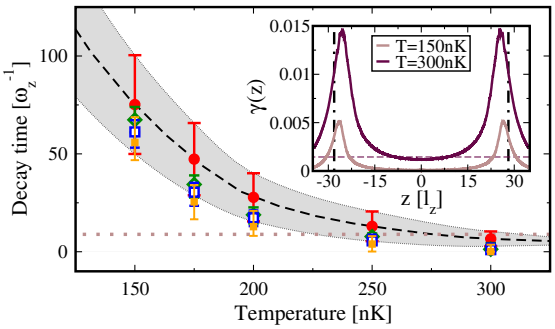

FIG. 2 (color online). Mean soliton decay times as a function of temperature obtained from 1D simulations of SGPE (red circles), DGPE with *ab initio* determined $\gamma(z)$ (green diamonds), and also *averaged* $\bar{\gamma}$ over $[-R/2, R/2]$ (blue hollow squares); 3D DGPE results corresponding to the latter (same axial density) are shown by orange filled squares. SGPE values within 1 standard deviation of the mean decay time (for 200 runs) are indicated by the grey band; the dotted horizontal line indicates one oscillation time for $T = 0$. Inset: $\gamma(z)$ (solid) for $T =$ 150 nK (bottom) and 300 nK with $\bar{\gamma}$ (horizontal) for $T =$ 300 nK; vertical lines show R (parameters as in Fig. 1; $T_\phi = N(\hbar\omega_z)^2/k_B\mu \approx 25$ nK [29], $T_c = N\hbar\omega_z/k_B \ln(2N) \approx 900$ nK [30]).

where $P(v)$ stands for the total perturbation, namely,

$$P(v) = \frac{1}{2\mu^2}\left[2(1-|v|^2)Vv + \frac{dV}{dz}\partial_z v + 2\gamma\mu\partial_t v\right], \qquad (5)$$

and all terms in P are assumed to be of the same order. We now apply the perturbation theory for matter-wave dark solitons [32]: starting from the soliton solution of the unperturbed system, we seek a solution in the form $v(z,t) = \cos\varphi(t)\tanh Z + i\sin\varphi(t)$, where $Z \equiv \cos\varphi(t)\times[z - z_0(t)]$, and $\varphi(t)$ and $z_0(t)$ are the slowly varying phase ($|\varphi| \le \pi/2$) and center of the soliton. The resulting equations for φ and z_0, namely, $d\varphi/dt = -(1/2)\cos\varphi dV/dz + (2/3)\gamma\mu\cos\varphi\sin\varphi$, and $dz_0/dt = \sin\varphi$, lead to the following equation of motion for the soliton center,

$$\frac{d^2z_0}{dt^2} = \left[\frac{2}{3}\gamma\mu\frac{dz_0}{dt} - \left(\frac{\Omega}{\sqrt{2}}\right)^2 z_0\right]\left[1 - \left(\frac{dz_0}{dt}\right)^2\right]. \qquad (6)$$

The nonlinear Eq. (6) can be integrated directly to yield the soliton trajectory: Fig. 3 shows very good agreement between the prediction of Eq. (6) (red) and the full DGPE (black) based on the spatially integrated $\bar{\gamma}$, which are also consistent with the SGPE predictions with $\gamma(z)$.

For a nearly black soliton (with $dz_0/dt \ll 1$), Eq. (6) reduces to the linear equation $d^2z_0/dt^2 - (2/3)\gamma\mu(dz_0/dt) + (\Omega/\sqrt{2})^2 z_0 = 0$. This includes the temperature-induced antidamping term $\propto -\gamma dz_0/dt$, and is reminiscent of the equation of motion derived by means of a kinetic theory approach [16]. For $T = 0$ ($\gamma = 0$) we recover the constant amplitude oscillation of frequency $\Omega/\sqrt{2}$ [14,32]. For $T \neq 0$ ($\gamma \neq 0$), the solutions of the linearized Eq. (6) are $z_0(t) = \exp(s_{1,2}t)z_0(0)$, where $s_{1,2} = \gamma\mu/3 \pm \sqrt{\Delta}(\Omega/\sqrt{2})$ are the roots of the resulting characteristic equation. The discriminant $\Delta \equiv (\gamma/\gamma_{\rm cr})^2 - 1$ (with $\gamma_{\rm cr} = (3/\mu)(\Omega/\sqrt{2}) = 0.053$ here) distinguishes the regimes of soliton trajectories as subcritical weak antidamping ($\Delta < 0$, $\gamma < \gamma_{\rm cr}$), critical ($\Delta = 0$, $\gamma = \gamma_{\rm cr}$), and supercritical strong antidamping ($\Delta > 0$, $\gamma > \gamma_{\rm cr}$). Assuming an initial soliton location $z_0(0) = 0$ and speed $\dot{z}_0(0)$, the subcritical soliton trajectory $z_0(t) = (\dot{z}_0(0)/\omega_o)\times e^{\gamma\mu t/3}\sin(\omega_o t)$, $\omega_o = (\Omega/\sqrt{2})\sqrt{1-(\gamma/\gamma_{\rm cr})^2}$, indicates an exponential increase in its maximum amplitude (Fig. 3 top, dashed green line), whose magnitude depends on both T and μ; the oscillation frequency ω_o is also shifted from its $T = 0$ value [13]. Corresponding trajectories in the critical and supercritical cases read $z_0(t) = \dot{z}_0(0)t\exp(\gamma\mu t/3)$ and $z_0(t) = [\dot{z}_0(0)/(s_1 - s_2)]\times[\exp(s_1 t) - \exp(s_2 t)]$. The above results are also supported by a linear stability analysis around the stationary dark soliton, $\psi_{\rm ds}$. This waveform makes the right-hand side of Eq. (2) vanish and is, thus, an exact solution of the $T \neq 0$ problem. The anomalous (negative Krein signature) mode of the soliton leads to an instability upon dissipative perturbations [33]: the relevant mode of the linearization around the soliton (solution of the eigenvalue problem

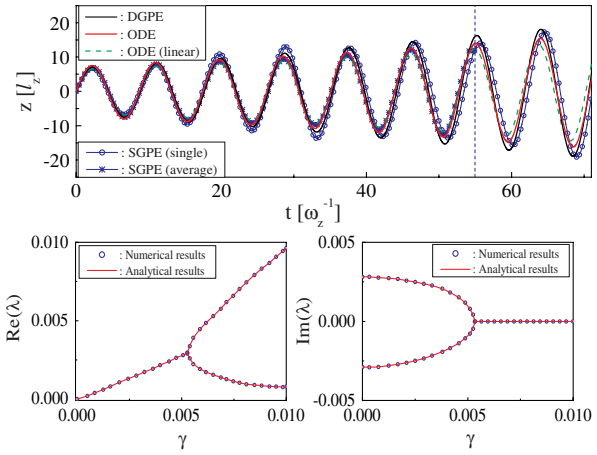

FIG. 3 (color online). Top: Soliton DGPE trajectory (black) vs analytical results (nonlinear: solid red; linear: dashed green) with $\gamma = \bar{\gamma} = 0.00014$, vs stochastic ones with $\gamma(z)$ (stars: 10-trajectory average, circles: single *mean-bin* trajectory). Bottom: Dependence of the real part (left; instability growth rate) and imaginary part (right; oscillation frequency) of the unstable eigenmode of the excitation spectrum on γ: analytical results (solid red) vs DGPE numerics (blue circles) ($T = 150$ nK.)

arising from $\psi = \psi_{\rm ds} + \epsilon(\exp(\lambda t)a(x) + \exp(\lambda^\star t)b^\star(x))$ for the eigenvalue-eigenvector pair $\{\lambda, (a, b)\}$) acquires $\mathrm{Re}(\lambda) > 0$ for $\gamma > 0$. Figure 3 (bottom) shows excellent agreement between the analytical prediction for the relevant eigenvalue and the numerical result for the DGPE excitation spectrum.

Discussion.—A full description of the rich features seen in dark soliton experiments, including shot-to-shot variations, requires a stochastic model incorporating density and phase fluctuations. The stochastic Gross-Pitaevskii equation was shown to capture these features well, leading to specific predictions for the spread of soliton decay times with different noise realizations, in close analogy to different experimental realizations. Nonetheless, mean soliton trajectories or decay times are captured reasonably by the simpler dissipative Gross-Pitaevskii equation (with additional experimental or theoretical input required). An analytical solution of the dark soliton motion in excellent agreement with the dissipative Gross-Pitaevskii equation was given, paving the way for future analytical studies of other macroscopic excitations in atomic condensates.

We acknowledge discussions with C. F. Barenghi and funding from EPSRC, NSF and S. A. R. G of U. of Athens.

[1] *Emergent Nonlinear Phenomena in Bose Einstein-Condensates*, edited by P. G. Kevrekidis, D. J. Frantzeskakis, and R. Carretero-Gonzalez (Springer, New York, 2008).
[2] W. H. Zurek, Phys. Rev. Lett. **102**, 105702 (2009); B. Damski and W. H. Zurek, arXiv:0909.0761v1.
[3] C. N. Weiler *et al.*, Nature (London) **455**, 948 (2008).
[4] T. W. B. Kibble, J. Phys. A **9**, 1387 (1976).
[5] W. H. Zurek, Phys. Rep. **276**, 177 (1996).
[6] Z. Dutton *et al.*, Science **293**, 663 (2001); P. Engels and C. Atherton, Phys. Rev. Lett. **99**, 160405 (2007).
[7] S. Burger *et al.*, Phys. Rev. Lett. **83**, 5198 (1999).
[8] J. Denschlag *et al.*, Science **287**, 97 (2000).
[9] C. Becker *et al.*, Nature Phys. **4**, 496 (2008).
[10] S. Stellmer *et al.*, Phys. Rev. Lett. **101**, 120406 (2008).
[11] A. Weller *et al.*, Phys. Rev. Lett. **101**, 130401 (2008).
[12] M. R. Matthews *et al.*, Phys. Rev. Lett. **83**, 2498 (1999); K. W. Madison *et al.*, Phys. Rev. Lett. **84**, 806 (2000).
[13] B. Jackson, N. P. Proukakis, and C. F. Barenghi, Phys. Rev. A **75**, 051601(R) (2007).
[14] Th. Busch and J. R. Anglin, Phys. Rev. Lett. **84**, 2298 (2000).
[15] I. V. Barashenkov, S. R. Woodford, and E. V. Zemlyanaya, Phys. Rev. Lett. **90**, 054103 (2003); N. P. Proukakis *et al.*, *ibid.* **93**, 130408 (2004).
[16] P. O. Fedichev, A. E. Muryshev, and G. V. Shlyapnikov, Phys. Rev. A **60**, 3220 (1999).
[17] J. Dziarmaga and K. Sacha, Phys. Rev. A **66**, 043620 (2002); A. Negretti, C. Henkel, and K. Molmer, Phys. Rev. A **77**, 043606 (2008); R. V. Mishmash *et al.*, arXiv:0906.4949v2; D. M. Gangardt and A. Kamenev, arXiv:0908.4513v1; C. K. Law, Phys. Rev. A **68**, 015602 (2003); A. D. Martin and J. Ruostekoski, arXiv:0909.2621v1.
[18] H. T. C. Stoof, J. Low Temp. Phys. **114**, 11 (1999); H. T. C. Stoof and M. J. Bijlsma, *ibid.* **124**, 431 (2001).
[19] C. W. Gardiner and M. J. Davis, J. Phys. B **36**, 4731 (2003).
[20] L. P. Pitaevskii, Zh. Eksp. Teor. Fiz. **35**, 408 (1958) [Sov. Phys. JETP **35**, 282 (1959)].
[21] S. Choi, S. A. Morgan, and K. Burnett, Phys. Rev. A **57**, 4057 (1998).
[22] M. Tsubota K. Kasamatsu, and M. Ueda, Phys. Rev. A **65**, 023603 (2002).
[23] Y. S. Kivshar *et al.*, Opt. Lett. **19**, 19 (1994); J. F. Corney and P. Drummond, J. Opt. Soc. Am. B **18**, 153 (2001).
[24] Z. Ivic *et al.*, Phys. Scr. **43**, 528 (1991); S. M. Alamoudi *et al.*, Phys. Rev. B **57**, 919 (1998).
[25] P. S. Lomdahl and W. C. Kerr, Phys. Rev. Lett. **55**, 1235 (1985); L. Cruzeiro, J. Biol. Phys. **35**, 43 (2009).
[26] S. Habib and G. Lythe, Phys. Rev. Lett. **84**, 1070 (2000).
[27] R. A. Duine and H. T. C. Stoof, Phys. Rev. A **65**, 013603 (2001); R. A. Duine, B. W. A. Leurs, and H. T. C. Stoof, Phys. Rev. A **69**, 053623 (2004); N. P. Proukakis, J. Schmiedmayer, and H. T. C. Stoof, *ibid.* **73**, 053603 (2006); N. P. Proukakis, Phys. Rev. A **74**, 053617 (2006).
[28] A. Muryshev *et al.*, Phys. Rev. Lett. **89**, 110401 (2002).
[29] D. S. Petrov, G. V. Shlyapnikov, and J. T. M. Walraven, Phys. Rev. Lett. **85**, 3745 (2000); U. Al Khawaja *et al.*, Phys. Rev. A **66**, 013615 (2002).
[30] W. Ketterle and N. J. van Druten, Phys. Rev. A **54**, 656 (1996).
[31] A. A. Penckwitt, R. J. Ballagh, and C. W. Gardiner, Phys. Rev. Lett. **89**, 260402 (2002).
[32] R. Carretero-González *et al.*, Nonlinearity **21**, R139 (2008).
[33] T. Kapitula *et al.*, Physica (Amsterdam) **195D**, 263 (2004).